R. & M. No. 2977
(17,060)
A.R.C. Technical Report

MINISTRY OF SUPPLY

AERONAUTICAL RESEARCH COUNCIL
REPORTS AND MEMORANDA

The Reflection Effect of Fences at Low Speeds

By

J. WEBER, DR.RER.NAT., and J. A. LAWFORD, B.Sc., A.F.R.AE.S.

LONDON: HER MAJESTY'S STATIONERY OFFICE
1956
PRICE 4s 6d NET

The Reflection Effect of Fences at Low Speeds

By

J. WEBER, DR.RER.NAT., and J. A. LAWFORD, B.Sc., A.F.R.AE.S.

COMMUNICATED BY THE PRINCIPAL DIRECTOR OF SCIENTIFIC RESEARCH (AIR),
MINISTRY OF SUPPLY

Reports and Memoranda No. 2977

*May, 1954**

Summary.—This note considers the effect on the flow over a swept wing, of vertical plates of small height—commonly called ' fences '. It is shown, as might be expected, that the nature of this effect is that of a partial-reflection plate. The effect of this partial reflection on the pressure distribution over the wing on either side of the fence has been investigated theoretically and by means of pressure measurements at low speeds on an untapered 45 deg swept-back wing.

An earlier physical explanation[1] of the flow changes caused by fences has been substantiated, and the proportion of full reflection effect has been determined experimentally for various shapes of fence. Methods are described for calculating the changes in pressures distribution, chordwise loading and spanwise loading.

The effect of a fence in obstructing boundary-layer outflow on swept-back wings of large aspect ratio has not been considered.

1. *Introduction.*—The peculiarities of the flow past swept wings at low speeds have made it necessary to consider in more detail the conditions which lead to a partial or a complete separation of the flow from the wing surface, and to the formation of part-span vortex sheets with their potentially highly undesirable effects on the pitching moment of the wing and on the downwash at the tail. Among various other devices, fences have in some cases proved to be effective in delaying the formation and modifying the form of part-span vortex sheets and thus in extending the usable lift range. A theoretical explanation of some ways in which such fences may operate physically is suggested in Ref. 1, and it is the purpose of the present note to substantiate this explanation experimentally and to provide a method of estimating their effect.

Only one aspect of the effect of fences is considered here: namely, that on thin swept wings where the breakdown of flow begins at the leading edge and occurs at low speeds. In this respect, according to Ref. 1, the main effect of the fence is to act as a partial-reflection plate, thus producing different pressure distributions and chordwise loadings on either side of it; it will also affect the shape of the sheet of trailing vortices and consequently the spanwise loading and the downwash at the tail. The modification of the spanwise loading due to the fences would tend to make the lift distribution more uniform for tapered swept-back wings and hence delay the formation of the part-span vortex sheets. The modification of the chordwise loading due to the fences would tend to reduce the suction peak outboard of the fence; this would slow down the inward movement of the part-span vortex sheets. The aim of the present investigation is to find out how large these effects are in a representative case and to what degree the changes in pressure on each side of the fence correspond to those expected from a reflection plate. This will lead to an approximate method for calculating the effect of a given fence on a given wing in inviscid incompressible flow.

* R.A.E. Tech. Note Aero. 2308, received 20th September, 1954.

The case of zero lift is also considered since a reflection effect will modify the velocity increments due to the thickness of the wing in a way which tends to reduce the critical Mach number over part of the wing surface.

Fences appear to have been used first by W. E. Gray (1935, *see* Ref. 2) and by P. Jordan[3], 1939, primarily in order to establish a fixed boundary between a part of a wing with attached flow and another part where the flow has broken down. In the absence of the fence, transverse fluctuations of the flow in the boundary between the two flow regimes have been observed on unswept wings and it has not yet been investigated whether similar fluctuations also occur on swept wings. For swept wings, fences have for some time been regarded solely as means of obstructing the spanwise drift of boundary-layer air. This effect is no doubt important on swept wings of large aspect ratio but it cannot explain the beneficial effect of fences on swept wings of moderate or small aspect ratios with leading-edge separations. It appears that the first use of the reflection effect of fences on swept wings has been made by R. Fail[4], 1947.

The present investigation does not consist of tests on a systematic series of wings with fences of various shapes and in different positions, nor is the actual breakdown of the flow over the leading edge near the fence studied. The only test made was to measure the pressure distribution in the junctions between wing and fence at small lift coefficients on a wing of moderate aspect ratio (where boundary-layer effects are small), and at a spanwise position where the pressure distribution in the absence of the fence is similar to that on an infinite sheared wing. An estimate of the effect of fences on other wings can then be obtained by calculation, the reflection effect being assumed to be additive.

2. *Details of Model and Tests.*—Pressure measurements were made in the No. 2, 11½-ft Wind Tunnel at the Royal Aircraft Establishment during August 1952 by Mrs. L. N. Illingworth; the tests were repeated with an improved model in August 1953 by the second author. The model used was the wing of aspect ratio 2 of the tests reported in Ref. 5 (*see* Fig. 1). It was swept-back 45 deg, untapered, of RAE 101 section 12 per cent thick and had a chord of 20 in. Curved leading-edge wing tips were fitted. Various fences (shown in Fig. 2) were placed immediately inboard and immediately outboard of a line of flush pressure holes at a distance of 0·42 of the semispan from the centre-line, since previous results show that there are only small centre and tip effects at this station, so that the pressure distribution in the absence of the fence is similar to that of a sheared wing of large span. Fences I, II and III extended forward of the leading edge by 0·05c (I) or 0·10c (II and III), were identical in shape on the upper and lower surfaces, and had elliptical noses which faired into a section parallel to the wing surface at 30 per cent chord. They were faired at the rear to meet the wing at the trailing edge. The fence height above the wing surface was 0·25, 0·50, and 0·75 of the maximum wing thickness for fences I, II and III respectively. Fence IIA was identical with fence II but with its rear end cut off at the maximum thickness position of the wing (*see* Fig. 2). Fence IIB was the same as fence II aft of 7·5 per cent chord, but forward of this point it was modified so as to extend only to the leading edge and to meet the wing surface at 0·75 per cent chord, as shown in Fig. 2. The fences were made of 18 gauge brass and, to avoid damaging the wing, were held on by brackets taped to the wing on the opposite side from the pressure holes. Pressure measurements were made on both surfaces at wing incidences of 0 deg, 3·1 deg, 7·1 deg and 11·2 deg. The windspeed was 163 ft/sec, giving a Reynolds number based on the wing chord of $1{\cdot}7 \times 10^6$, in order to conform with previous measurements[5] on this wing.

3. *Effects at Zero Lift.*—The measured pressure distributions in the inboard and outboard junctions between fence and wing have been plotted in Fig. 3. For comparison, the pressure distribution of the wing alone at that station is also shown. The changes of pressure due to even the smallest of the fences is strikingly large. To obtain similar changes from a modification of the leading edge of the section would require considerable changes of the section shape. The fence thus proves to be an extremely effective means of influencing the local pressure distribution on swept wings.

That the changes of the pressure distribution are related to those obtained from reflection plates, or at the centre of swept wings, can be seen from Fig. 4, where the curve ' full reflection outboard ' gives the pressure distribution measured at the centre of the wing alone, and the curve ' full reflection inboard ' the pressure distribution measured in the ' swept-forward ' junction of the wing with a very large reflection plate (of height equal to the wing chord), the wing being of large aspect ratio in both cases but with the same section and angle of sweep. To show the modifications more clearly, the difference between the distorted distributions and that on the wing alone (*i.e.*, sheared-wing distribution) has been plotted in Fig. 4.

Analytically, the full reflection, or centre, effect can be expressed as an additional term to that giving the distribution over a section of an infinite sheared wing (*see e.g.*, Ref. 6). The similarity to a centre distribution found experimentally for the fence distributions can, therefore, be expressed as a factor, ε_0, to the centre term.

$$C_p = 1 - \frac{\{1 + \cos\varphi \,.\, S^{(1)}(x) - \varepsilon_0 f(\varphi) \cos\varphi \,.\, S^{(2)}(x)\}^2}{1 + [S^{(2)}(x)]^2} \qquad \ldots \qquad \ldots \qquad (1)$$

where x is the distance from the leading edge in terms of the local wing chord; $S^{(1)}(x)$ and $S^{(2)}(x)$ are functions of x dependent only on the section shape; and

$$f(\varphi) = \frac{1}{\pi} \ln \frac{1 + \sin\varphi}{1 - \sin\varphi},$$

as in Ref. 6. It remains to find empirical values for ε_0 from the experiments.

It is to be expected that ε_0 will depend primarily on the size of the fence, for which the ratio between the fence height outside the section to the maximum wing thickness, H/t, is a convenient measure. To a lesser extent, ε_0 will also depend on the actual shape of the fence. It will be seen from Fig. 4 that ε_0 is not really constant along the chord: there is less of a reflection effect behind the maximum thickness of the wing than ahead of it*. Therefore, a mean value for ε_0 is introduced, which can be obtained by comparing the tangential force coefficient.

$$C_T = \oint C_p \, d\left(\frac{z}{c}\right)$$

for each fence with the C_T value measured for full reflection (inboard or outboard as appropriate):

$$\varepsilon_0 = \frac{C_{T\ \text{With fence}}}{C_{T\ \text{Full reflection}}} \,. \qquad \ldots \qquad \ldots \qquad \ldots \qquad \ldots \qquad \ldots \qquad \ldots \qquad \ldots \qquad (2)$$

This is a convenient measure of the fence effect since, without reflection, $C_T = 0$ for inviscid flow** so that a non-zero value of C_T can arise only from the centre term $\varepsilon_0 f(\varphi) \cos\varphi \,.\, S^{(2)}(x)$ in equation (1). From equation (2), $\varepsilon_0 = 1$ for full reflection, and $\varepsilon_0 = 0$ if there is no reflection effect.

Experimental values of ε_0 have been plotted in Fig. 5. The value of ε_0 increases with H/t and approaches unity when the height of the fence outside the wing is of the order of the wing thickness There appears to be less of a reflection effect in the outboard junction than in the inboard junction. This, however, is due to a secondary effect of the boundary layer on the fence, which leads to different values of the pressure at the leading edge of the wing where stagnation pressure would have been obtained in inviscid flow. Because of the asymmetry of the flow about the fence upstream of the leading edge, $C_p = +0{\cdot}88$ inboard and $C_p = +0{\cdot}59$ outboard of fence II. The reflection effect, as obtained from equation (2), is apparently reduced if $C_p < 1$ at that point, and the curve obtained for the inboard side of the fence in Fig. 5 should, therefore, be the more representative.

* The characteristic ' dip ' in the pressure distribution, mainly in the outboard junction, Fig. 3 around $x/c = 0{\cdot}6$, presumably indicates transition from laminar to turbulent flow.

** In viscid flow, $C_T \neq 0$ for the sheared wing. In order to obtain $\varepsilon_0 = 0$ for no reflection effect, the value of C_T as measured for the wing alone has always been subtracted.

The experimental pressure distributions for fences II and III are compared with those calculated with $\varepsilon_0 = 0{\cdot}8$ in Fig. 6. There is fair agreement for points upstream of the maximum wing thickness, except for points very close to the leading edge where very high suction peaks occur; behind the maximum thickness, the calculation overestimates the reflection effect, as is to be expected. It would be simple enough to let ε_0 vary with x by letting it depend on the local ratio $H(x)/t(x)$, but to determine this relationship would require more detailed measurements.

The spanwise decrease of the reflection effect on either side of the fence has not been measured As the fence effect is so closely related to the ordinary centre effect, it can be assumed that its fading-out can be estimated in the same way as that of the centre effect, which has been explained in Ref. 6. The fence effect will then disappear at a spanwise distance of about half the local wing chord on either side of the fence.

Some of the experiments concerned the effect of the actual shape of the fence. It was found, in the first instance, that removing the lower part of the fence left the pressures in the upper junction practically unaltered whereas the pressures on the lower surface were very nearly the same as those with no fence at all. Cutting away the rear part of the fence behind maximum thickness (fence IIA, Figs. 3 and 4) left the pressures in the front part as they were with the whole fence. Hence, a fence which is meant to affect the pressures only over the leading-edge part of the upper surface of an aerofoil needs to extend only over that part of the aerofoil, *i.e.*, the fence can be cut off soon behind the stagnation point on the lower surface and behind maximum thickness on the upper surface. To extend the fence over the region of the stagnation point is quite essential, however, as can be seen from the results for fence IIB in Figs. 3 and 4. The reflection effect of the fence is severely diminished by the cut-out near the nose.

To show that plates or bodies of small chordwise extent, protruding from the wing surface, can still be regarded as reflection plates, the results from another test may be mentioned here; this concerned a 40-deg swept-back wing of $8{\cdot}5$ per cent thickness/chord ratio with a strut of $8{\cdot}5$ per cent thickness/chord ratio, swept forward by 45 deg, attached to the lower surface, its chord being about a quarter of the wing chord.[7] An estimate of the pressure distributions along the strut-wing junctions has been made by assuming that the strut acted as a full reflection plate over that part of the wing chord where the strut is situated. This gives different values on either side of the strut since the wing was swept. To these the increments arising from the strut alone are added (in this case by taking the junction as the centre-section of a swept-forward wing of infinite aspect ratio). The resultant pressure distributions are in good agreement with the measured values, as can be seen from Fig. 7.

4. *The Chordwise Loading.*—As the fence acts as a partial-reflection plate to the source lines representing the thickness of the wing, it should similarly react upon the bound vortices representing the lift on the wing. This means a redistribution of the lift along the chord, similar to that found at the centre of swept wings[8]. As a consequence of this change of chordwise loading, the pressure distribution along the surface, the sectional lift slope, a, and the chordwise position of the aerodynamic centre are affected by the presence of the fence.

Measured chordwise loadings in the form of differences between the pressure coefficients of the upper and lower surfaces in the junctions are plotted in Figs. 8, 9 and 10 against $\sqrt{(x/c)}$ in order to show more clearly the changes near the leading edge by stretching the co-ordinate there. Comparison with calculated curves for full reflection, from Refs. 8 and 9 (for the same sectional lift coefficient C_L as for the wing alone at the fence position), show that the reflection effect is very marked. There are considerable load (and thus suction) peaks in the inboard junctions near the leading edge, similar to those at the centre of a swept-forward wing; and a considerable reduction of the load (and thus of the suction) near the leading edge of the outboard junction. The latter is one of the main beneficial effects of a fence because it should postpone the separation of the flow there and thus delay the inward movement of the part-span vortex sheets[1].

To express the presence of a reflection effect analytically, the parameter n in the expression

$$\Delta C_p = -\frac{\sin \pi n}{\pi n} C_L \left(\frac{1-x}{x}\right)^n \quad .. \quad .. \quad .. \quad .. \quad .. \quad .. \quad (3)$$

for the chordwise loading on a thin wing[8] must be varied, and we put

$$n = 1 - \frac{1 + \lambda \frac{\varphi_e}{\pi/2} + \varepsilon_\alpha \lambda_F \frac{\varphi_e}{\pi/2}}{2\left\{1 + \left(\frac{a_0 \cos \varphi_e}{\pi A}\right)^2\right\}^{\frac{1}{4\left(1 + \frac{|\varphi_e|}{\pi/2}\right)}}}, \quad .. \quad .. \quad .. \quad .. \quad (4)$$

where φ_e is the effective angle of sweep of the wing and A its aspect ratio. λ is an interpolation function, with values between 0 and ± 1, for the ordinary centre and tip effects of the wing. The new term is

$$\varepsilon_\alpha \lambda_F \frac{\varphi_e}{\pi/2},$$

where $\lambda_F(y/c)$ is another interpolation function with $\lambda_F = +1$ on the outboard (swept-back) side of the fence and $\lambda_F = -1$ on the inboard (swept-forward) side, and tending to zero on either side of the fence as the distance increases. The value of λ_F can be taken as being the same function of y/c as $\lambda(y/c)$ which is explained in Ref. 8. ε_α is a reflection factor for the lift term, corresponding to ε_0 for the thickness term.

It is convenient to find a mean value of ε_α from the experiments. The simplest way is to determine the shift, $\Delta x_{\text{a.c.}}$, of the chordwise position of the aerodynamic centre due to the fence, which is related to ε_α by

$$\Delta x_{\text{a.c.}} = \varepsilon_\alpha \lambda_F(y) \frac{\varphi_e}{\pi/2}$$

for wings of large aspect ratio, as explained in Ref. 8, so that, for the junctions,

$$\varepsilon_\alpha = \pm \frac{\Delta x_{\text{a.c.}}}{\frac{\varphi_e}{\pi/2}} \quad .. \quad .. \quad .. \quad .. \quad .. \quad .. \quad .. \quad .. \quad (5)$$

to a first approximation. The results of such an analysis for fences I, II and III are shown in Fig. 11. There is again slightly less reflection effect in the outboard junction than in the inboard junction.

To obtain the pressure distribution along the junction, including higher-order terms for thickness and lift, we have from Ref. 9:

$$C_p = 1 - \frac{\left\{\cos \alpha_e [1 + \cos \varphi \,.\, S^{(1)}(x) - \varepsilon_0 f(\varphi) \cos \varphi \,.\, S^{(2)}(x)] \pm \sin \alpha_e \cos \varphi \left(\frac{1-x}{x}\right)^n [1 + S^3(x)]\right\}^2}{1 + [S^{(2)}(x)]^2}, \quad (6)$$

the alternative positive and negative signs applying to the upper and lower surfaces respectively. By taking the differences between the surfaces, we obtain:

$$\Delta C_p = -4 \cos \alpha_e \sin \alpha_e \cos \varphi \left(\frac{1-x}{x}\right)^n \frac{[1 + \cos \varphi S^{(1)}(x) - \varepsilon_0 f(\varphi) S^{(2)}(x)][1 + S^{(3)}(x)]}{1 + [S^{(2)}(x)]^2}, \quad .. \quad .. \quad (7)$$

where, in addition to the quantities defined above, α_e is the effective angle of incidence and $S^{(3)}(x)$ a further function of x dependent on the section shape and defined in Ref. 9.

In Fig. 12, a comparison is made between measured pressure distributions in the junctions and values calculated from equation (6), using the mean values for ε_α from Fig. 11. The calculated result will be sufficiently accurate for most practical purposes. In order to obtain the peak values it appears to be preferable not to use a mean value of ε_α over the whole chord but to assume full reflection (*i.e.*, $\varepsilon_\alpha = 1$) for points very close to the leading edge and for fences that extend around the leading edge. This is also shown by the results in Figs. 6 and 8.

The conclusions drawn so far apply to a flow at small or moderate lift coefficients. As the lift increases, boundary-layer effects and flow separations appeared in the experimental results and can be expected to appear to some extent also at full-scale Reynolds numbers. The order of the disturbances due to viscosity can be seen from Fig. 9. The main feature is a premature separation of the flow from the inboard junction; but this need not be detrimental to the purpose of a fence, as explained in Ref. 1. Fortunately, there is no sign of any large effect of viscosity in the outboard junction.

As in the case without lift, the rear end of the fence can be omitted without affecting the pressure distribution near the leading edge much (*see* fence IIA in Fig. 10). But a cut-out, as for fence IIB, nearly destroys the beneficial effect in the outboard junction, producing a suction peak, however, further back in the inboard junction where it is not wanted.

5. *The Spanwise Loading.*—A fence affects the spanwise loading in two ways:

   (*a*) The sectional lift slope, a, differs from that of the wing alone because of the change in chordwise loading; the value of a jumps from a higher value in the inboard junction (for a swept-back wing) to a lower value in the outboard junction. Thus the effective incidence $\alpha_e = C_L/a$ is affected.

   (*b*) The fence leaves a trace of free vortices in the wake behind the wing because a sudden change in chordwise loading is possible only if some of the bound vortices inboards continue along the fence (which thus carries a sideforce) and subsequently leave the fence and not the wing trailing edge as trailing vortices. Thus the induced incidence from the system of trailing vortices is affected.

The problem of calculating the load distribution over a wing with discontinuities in the sectional lift slope and with a sheet of trailing vortices like that produced by the fences has been treated in Ref. 10. It was found that the change of the sectional lift slope due to a fence has very little effect on the spanwise loading so that, in calculating this, the variation of a may be ignored. The spanwise loading is, however, appreciably affected by the shape of the trailing vortex sheet.

Using the method of Ref. 10, the spanwise loading has been calculated for the wing with fence II, and the result is compared with the measured values in Fig. 13. In addition to the load of the wing alone (calculated from Ref. 8), a load $\Delta C_L(y)$ can be calculated, which depends on the spanwise position of the fence and on the ratio between fence height and wing span, h/b. To a first approximation we may put

$$\frac{h}{b} = \frac{2H + t}{b} = \left(2\frac{H}{t} + 1\right)\frac{t}{c} \cdot \frac{c/\bar{c}}{A} \qquad \ldots \quad \ldots \quad \ldots \quad \ldots \quad \ldots \quad (8)$$

and take the value of H/t at the maximum thickness of the section. This gives $h/b = 0{\cdot}12$ for fence II. It will be seen from Fig. 13 that the jump in lift at the fence is adequately represented by the calculation for low incidences. As the incidence increases, boundary effects reduce the lift in the junctions; naturally more so in the inboard than in the outboard junction. Again, there is a greater lift reduction in the inboard junction than on the wing alone because the boundary layer can be expected to be thicker there than on the wing alone, and because flow separation occurs earlier. Thus, at high incidences, a dip in the spanwise lift distribution near the fence is sometimes observed in tunnel tests. This is, however, subject to scale effect and it can be expected that, at full-scale Reynolds number, the lift distribution is more like the calculated one also at high incidences below the stall.

The jump in lift is equal to a sideforce on the fence. The distribution of the sideforce along the height of the fence follows approximately an ellipse, as shown in Ref. 10. The local sideforces at the base of the fence can, of course, be obtained from the pressure differences in the junctions.

6. *Conclusions.*—At zero lift, a fence on a swept-back wing acts as a partial-reflection plate, producing a pressure distribution similar to that of a swept-forward wing inboard of the fence and of a swept-back wing outboard of the fence. The magnitude of the effect depends on the height of the fence in relation to the thickness of the section and the reflection factor ε_0 is between a half and unity for a typical size of fence in use at present (Fig. 5). This effect may be detrimental at high Mach numbers.

With the wing at incidence, a fence has similar reflection effects on the bound vortices, causing high suction peaks inboard and reduced peaks outboard of the fence. The proportion of full reflection effect, taken as a mean along the whole chord, varies between a quarter and a half, according to the fence height; pronounced peaks near the leading edge tend to show the full reflection effect, if the fence extends around the leading edge. A method is suggested for calculating the pressure distribution for a wing with fence.

The spanwise loading is mainly affected by the modified sheet of trailing vortices. The lift is increased between the fences and reduced outside them. The change in load distribution can be calculated by using the method of Ref. 10, as long as no flow separations occur.

In designing fences to improve the leading-edge stall at low speeds, the first step should be to calculate the spanwise loading with various fence arrangements for the given wing. Although the change of the span loading is generally small, it may be possible, for wings of moderate sweep and taper, to convert a span loading curve which leads to tip stalling into one where the first breakdown occurs near the middle of the wing, possibly by using more than one pair of fences. The calculation of the pressure distributions in the junctions and some knowledge of the formation and movement of the part-span vortices on the wing without fences are needed to decide on a suitable spanwise position of the fences and on their height. The main gap in knowledge to effect such a design is that there is at present no reliable criterion for deciding what pressure distribution is permissible in order to avoid flow separations with long bubbles or completely broken-down flow. Although the suction peaks can give some guidance as to the improvements obtainable from fences, much further work is needed before a completely rational design of fences can be made.

The calculation methods described above can be extended to apply also to subcritical compressible flow, as explained in Ref. 8, but even less is known in this speed range as to what constitutes desirable design features.

LIST OF SYMBOLS

x, y	Rectangular co-ordinates; x along the main stream, $x = 0$ at the leading edge, y in the spanwise direction
c	Local wing chord
$\bar{c}$	Mean wing chord
b	Wing span
t	Maximum thickness
H	Height of fence above the wing surface
h	Height of trailing vortex sheet
φ	Angle of sweep
α	Geometric incidence
α_i	Effective incidence
C_p	Pressure coefficient
ΔC_p	Difference between pressure coefficients on upper and lower surface
C_L	Lift coefficient
C_T	Tangential force coefficient
a	Sectional lift slope, *see* Ref. 8
$\Delta x_{a.c.}$	Shift of the chordwise position of the aerodynamic centre
ε_0	Reflection factor for thickness effects
ε_α	Reflection factor for lift effects
n	Parameter for the chordwise loading, *see* Ref. 8
$\lambda(y)$	Interpolation function, *see* Ref. 8
$S^{(1)}(x), S^{(2)}(x), S^{(3)}(x)$	Functions of section shape, *see* Ref. 9

REFERENCES

No.	*Author*	*Title, etc.*
1	D. Küchemann	Types of flow on swept wings, with special reference to free boundaries and vortex sheets. *J.R.Ae.Soc.* Vol. 57, p. 683. November, 1953.
2	H. B. Irving, J. H. Warsap and H. J. Gummer.	Model experiments on Gray stabilizer fins. A.R.C. 2112. November, 1935.
3	P. Jordan	Auftriebsberechnung und Strömungsvorgänge beim Ueberschreiten des Maximalauftriebes. *L.F.F.* Vol. 16, p. 184. 1939.
4	R. Fail	Effect of tail height and of inset nose fins on the longitudinal stability near the stall of an aircraft with sweptback wing. R.A.E. Tech. Note Aero. 1916. A.R.C. 10,956. September, 1947.
5	D. Küchemann, J. Weber and G. G. Brebner.	Low-speed tests on wings of 45 deg sweep. Part II: Balance and pressure measurements on wings of different aspect ratio. R. & M. 2882. May, 1951.
6	D. Küchemann and J. Weber	The subsonic flow past swept wings at zero lift without and with body. R. & M. 2908. March, 1953.
7	Wind Tunnel Staff, Low Speed Tunnels, R.A.E.	Low speed tunnel tests on drop tanks on sweptback wings. R.A.E. Report Aero. 2387. July, 1950.
8	D. Küchemann	A simple method of calculating the span- and chordwise loading on straight and swept wings of any given aspect ratio at subsonic speeds. R. & M. 2935. August, 1952.
9	J. Weber	The calculation of the pressure distribution over the surface of two-dimensional and swept wings with symmetrical aerofoil section. R. & M. 2918. July, 1953.
10	J. Weber	Theoretical load distribution on a wing with vertical plates. R. & M. 2960. March, 1954.

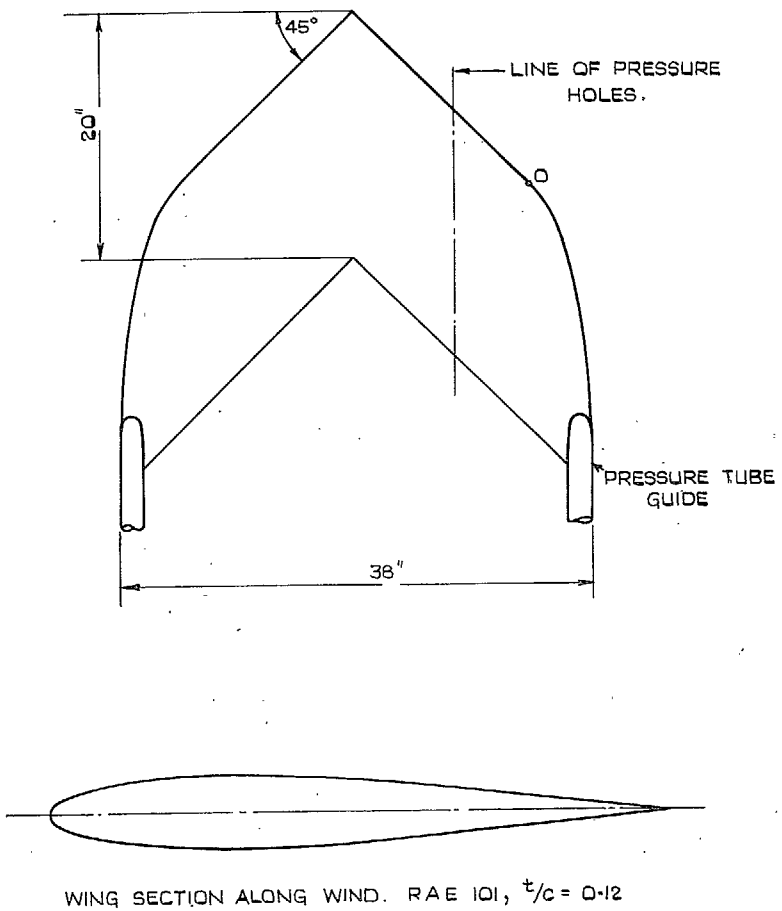

FIG. 1. General arrangement of wing.

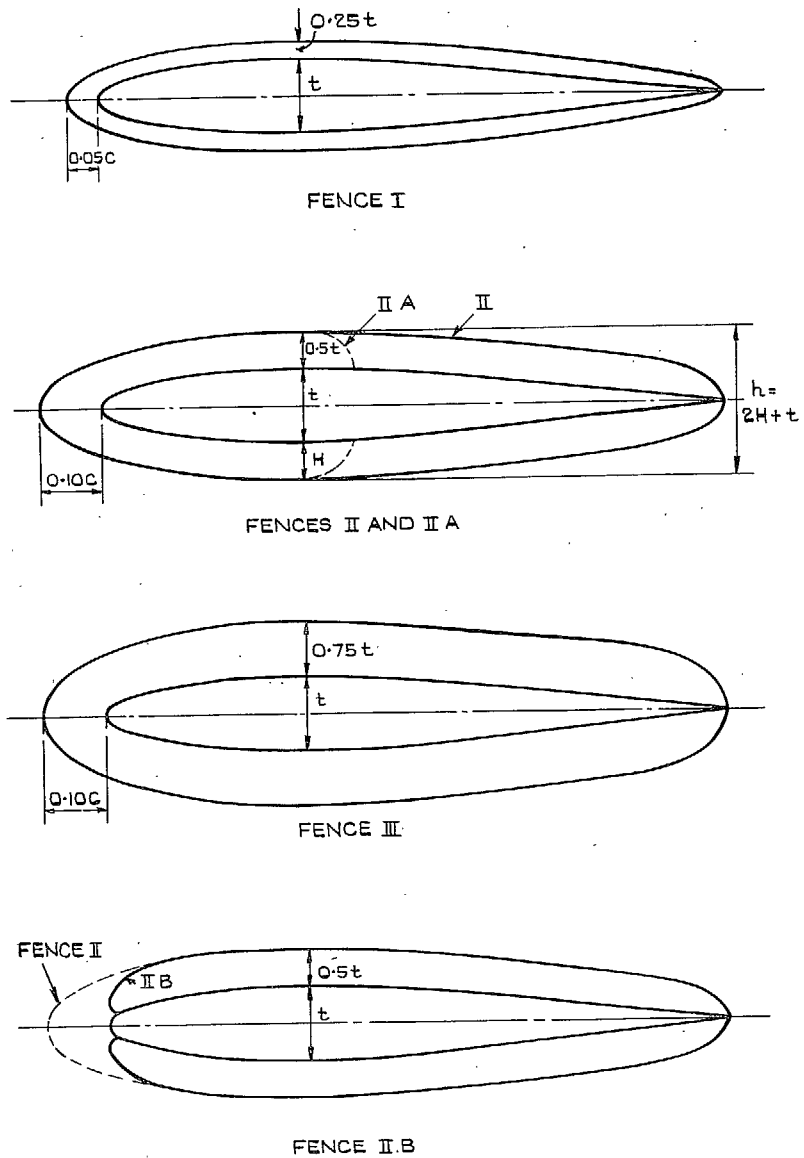

FIG. 2. Details of fences.

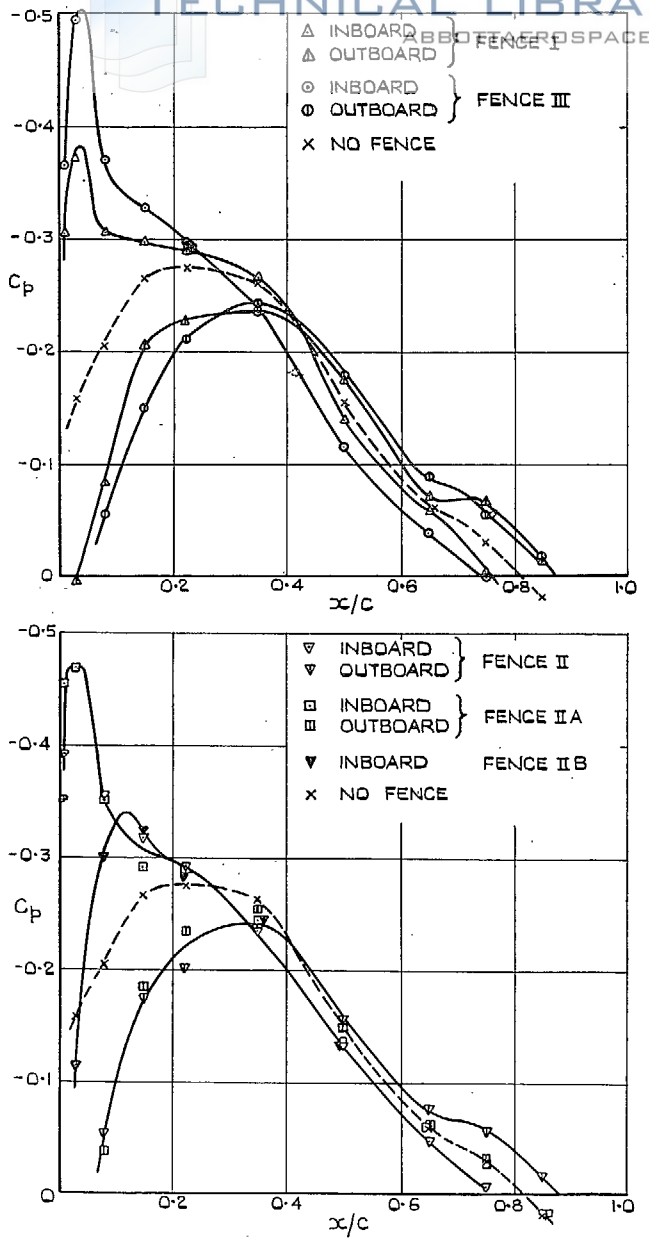

FIG. 3. Measured pressure distributions in the junctions between wing and fences at zero incidence.

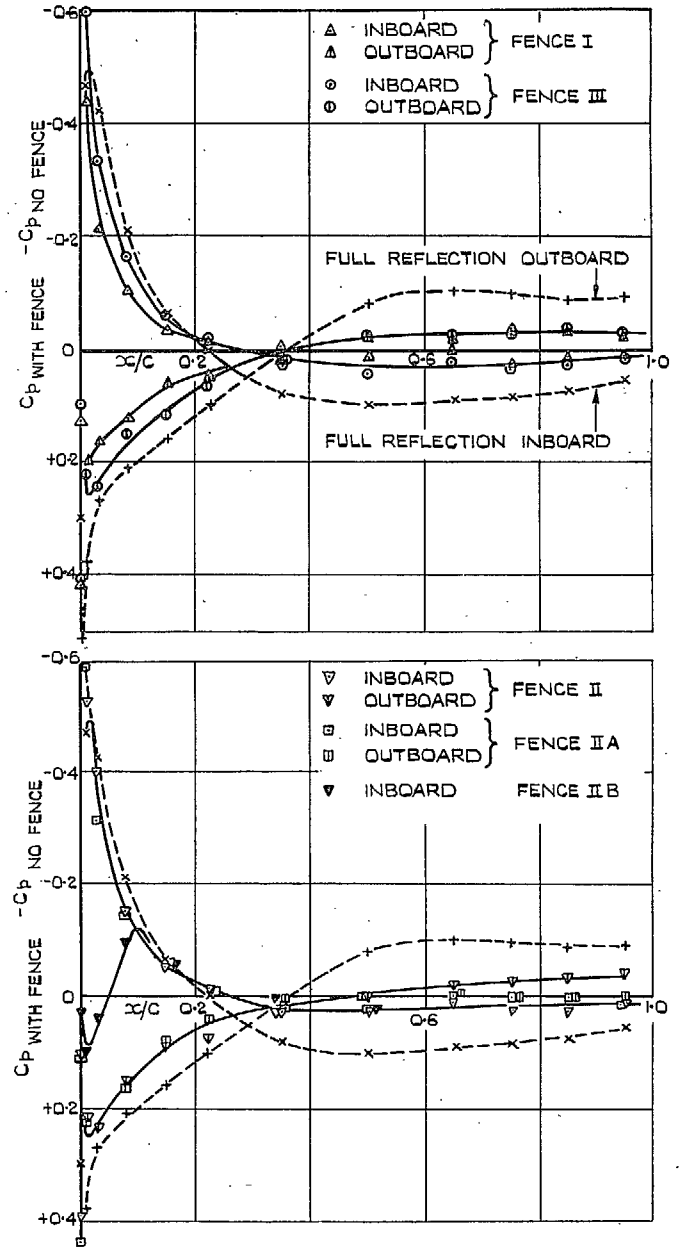

FIG. 4. Measured pressure differences in the junctions due to fences, at zero incidence.

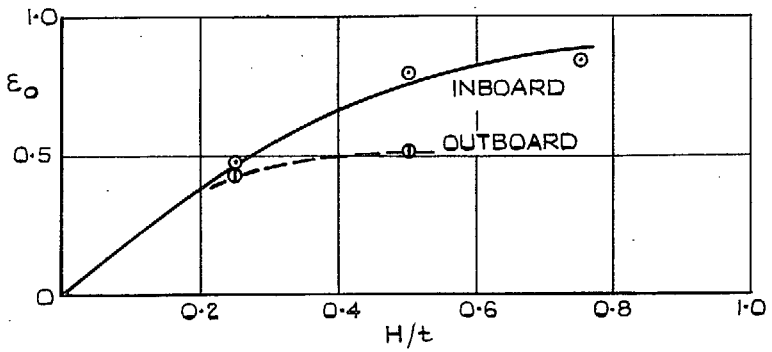

FIG. 5. Reflection factor for thickness effects, from data for fences I, II and III.

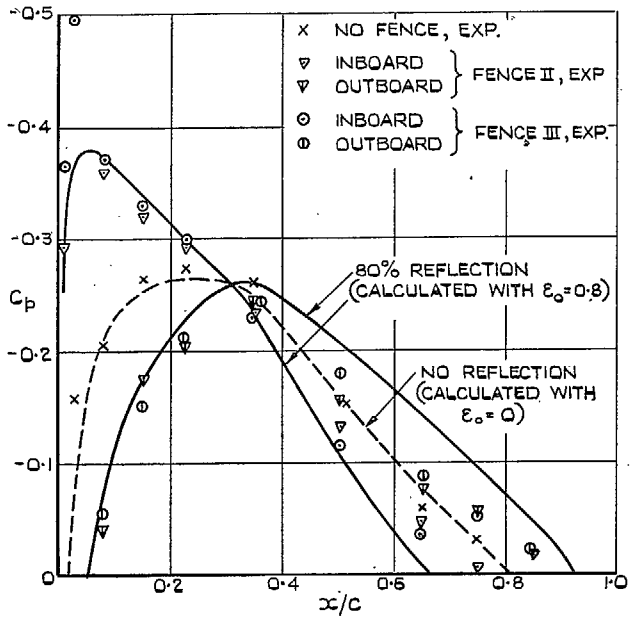

FIG. 6. Comparison between measured and calculated pressure distributions in the junctions at zero incidence.

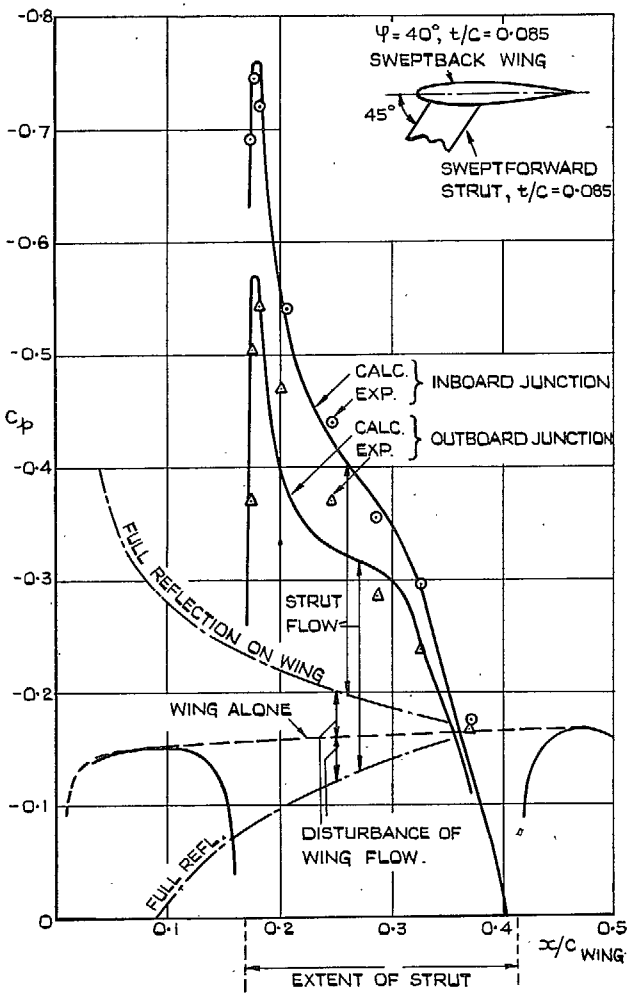

FIG. 7. Comparison between measured and calculated pressure distributions in the junctions between a swept-back wing and a swept-forward strut at zero incidence.

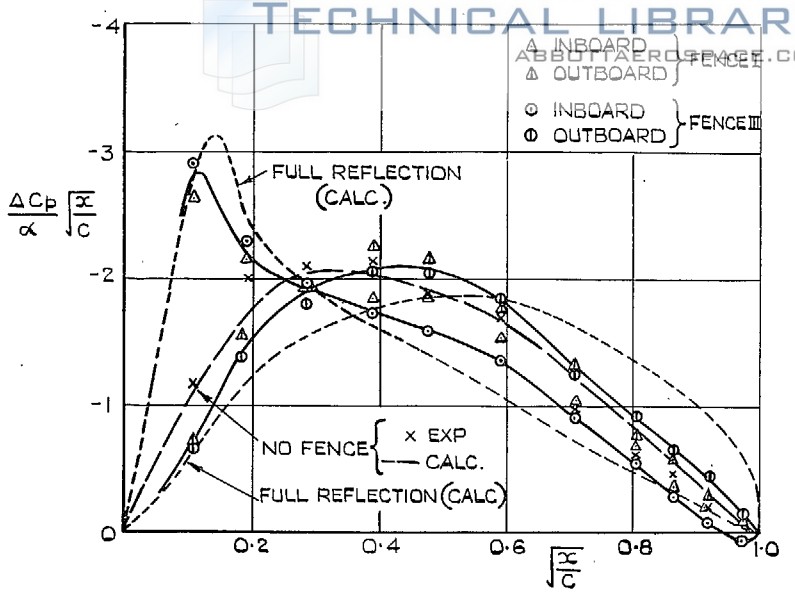

FIG. 8. Measured chordwise loadings in the junctions between wing and fences at $\alpha = 3{\cdot}1$ deg.

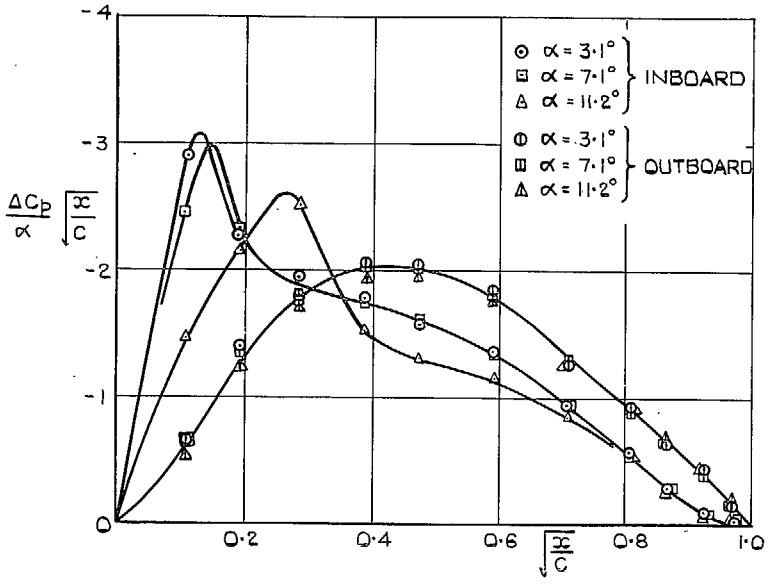

FIG. 9. Measured chordwise loadings in the junctions between wing and fence III at various incidences.

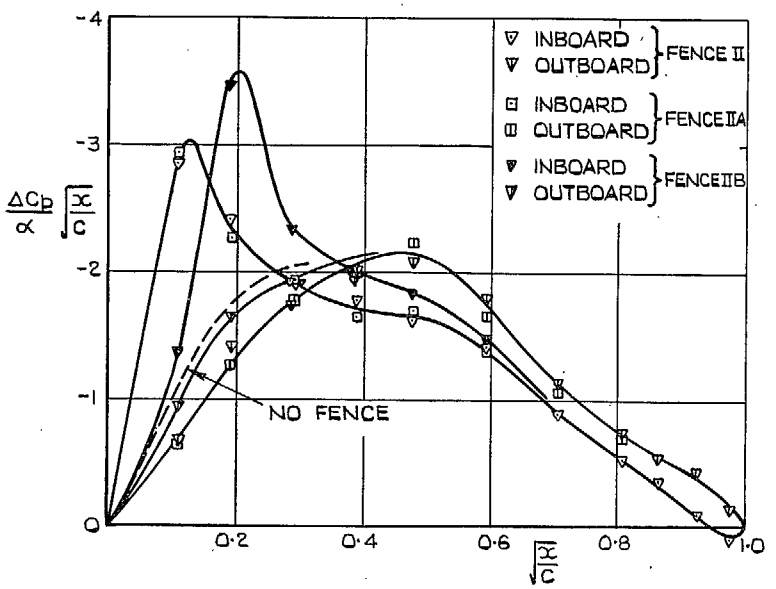

FIG. 10. Measured chordwise loadings in the junctions between wing and fences at $\alpha = 3{\cdot}1$ deg.

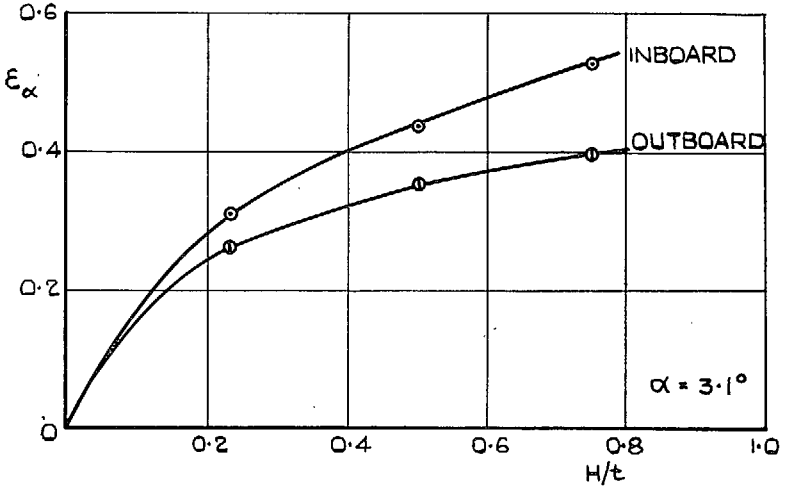

FIG. 11. Reflection factor for lift effects, from data for fences I, II, and III.

4279) Wt. 19/8411 K7 12/56 Hw.

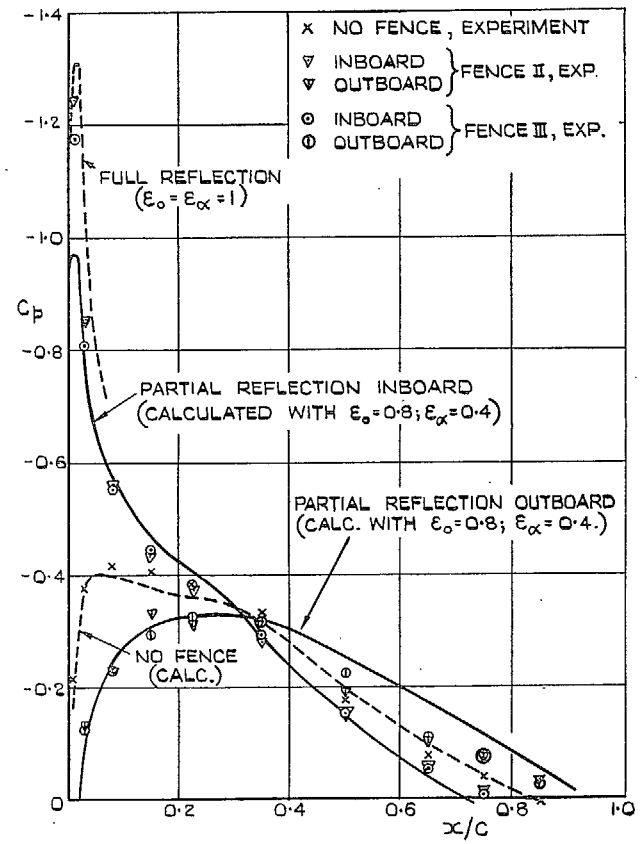

FIG. 12. Comparison between measured and calculated pressure distributions in the junctions at $\alpha = 3{\cdot}1$ deg.

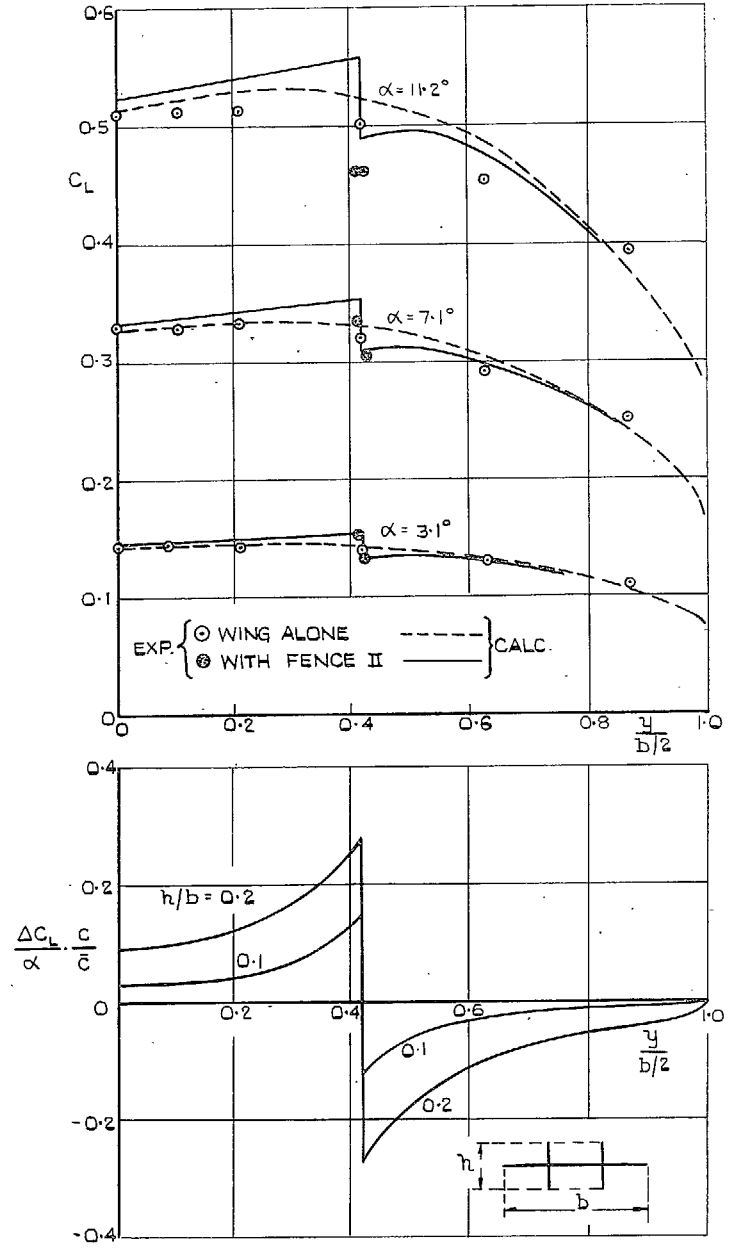

FIG. 13. Measured and calculated spanwise load distributions.

Publications of the Aeronautical Research Council

ANNUAL TECHNICAL REPORTS OF THE AERONAUTICAL RESEARCH COUNCIL (BOUND VOLUMES)

1939 Vol. I. Aerodynamics General, Performance, Airscrews, Engines. 50*s.* (51*s.* 9*d.*).
Vol. II. Stability and Control, Flutter and Vibration, Instruments, Structures, Seaplanes, etc. 63*s.* (64*s.* 9*d.*)

1940 Aero and Hydrodynamics, Aerofoils, Airscrews, Engines, Flutter, Icing, Stability and Control Structures, and a miscellaneous section. 50*s.* (51*s.* 9*d.*)

1941 Aero and Hydrodynamics, Aerofoils, Airscrews, Engines, Flutter, Stability and Control Structures. 63*s.* (64*s.* 9*d.*)

1942 Vol. I. Aero and Hydrodynamics, Aerofoils, Airscrews, Engines. 75*s.* (76*s.* 9*d.*)
Vol. II. Noise, Parachutes, Stability and Control, Structures, Vibration, Wind Tunnels. 47*s.* 6*d.* (49*s.* 3*d.*)

1943 Vol. I. Aerodynamics, Aerofoils, Airscrews. 80*s.* (81*s.* 9*d.*)
Vol. II. Engines, Flutter, Materials, Parachutes, Performance, Stability and Control, Structures. 90*s.* (92*s.* 6*d.*)

1944 Vol. I. Aero and Hydrodynamics, Aerofoils, Aircraft, Airscrews, Controls. 84*s.* (86*s.* 3*d.*)
Vol. II. Flutter and Vibration, Materials, Miscellaneous, Navigation, Parachutes, Performance, Plates and Panels, Stability, Structures, Test Equipment, Wind Tunnels. 84*s.* (86*s.* 3*d.*)

1945 Vol. I. Aero and Hydrodynamics, Aerofoils. 130*s.* (132*s.* 6*d.*)
Vol. II. Aircraft, Airscrews, Controls. 130*s.* (132*s.* 6*d.*)
Vol. III. Flutter and Vibration, Instruments, Miscellaneous, Parachutes, Plates and Panels, Propulsion. 130*s.* (132*s.* 3*d.*)
Vol. IV. Stability, Structures, Wind Tunnels, Wind Tunnel Technique. 130*s.* (132*s.* 3*d.*)

Annual Reports of the Aeronautical Research Council—

1937 2*s.* (2*s.* 2*d.*) 1938 1*s.* 6*d.* (1*s.* 8*d.*) 1939–48 3*s.* (3*s.* 3*d.*)

Index to all Reports and Memoranda published in the Annual Technical Reports, and separately—

April, 1950 - - - - R. & M. 2600 2*s.* 6*d.* (2*s.* 8*d.*)

Author Index to all Reports and Memoranda of the Aeronautical Research Council—

1909—January, 1954 R. & M. No. 2570 15*s.* (15*s.* 6*d.*)

Indexes to the Technical Reports of the Aeronautical Research Council—

December 1, 1936—June 30, 1939	R. & M. No. 1850	1*s.* 3*d.* (1*s.* 5*d.*)
July 1, 1939—June 30, 1945	R. & M. No. 1950	1*s.* (1*s.* 2*d.*)
July 1, 1945—June 30, 1946	R. & M. No. 2050	1*s.* (1*s.* 2*d.*)
July 1, 1946—December 31, 1946	R. & M. No. 2150	1*s.* 3*d.* (1*s.* 5*d.*)
January 1, 1947—June 30, 1947	R. & M. No. 2250	1*s.* 3*d.* (1*s.* 5*d.*)

Published Reports and Memoranda of the Aeronautical Research Council—

Between Nos. 2251–2349	R. & M. No. 2350	1*s.* 9*d.* (1*s.* 11*d.*)
Between Nos. 2351–2449	R. & M. No. 2450	2*s.* (2*s.* 2*d.*)
Between Nos. 2451–2549	R. & M. No. 2550	2*s.* 6*d.* (2*s.* 8*d.*)
Between Nos. 2551–2649	R. & M. No. 2650	2*s.* 6*d.* (2*s.* 8*d.*)

Prices in brackets include postage

HER MAJESTY'S STATIONERY OFFICE

York House, Kingsway, London W.C.2; 423 Oxford Street, London W.1 (Post Orders: P.O. Box 569, London S.E.1)
13a Castle Street, Edinburgh 2; 39 King Street, Manchester 2; 2 Edmund Street, Birmingham 3; 109 St. Mary Street, Cardiff; Tower Lane, Bristol, 1; 80 Chichester Street, Belfast, *or through any bookseller.*

S.O. Code No. 23-2977